5-1-2019

STEERING AND SUSPENSION DESIGN FOR AN EFFICIENT ELECTRIC DRIVE SYSTEM

Matthew Smith

STEERING AND SUSPENSION DESIGN
FOR AN EFFICIENT ELECTRIC
DRIVE SYSTEM

by

MATTHEW SMITH

Presented to the Faculty of the Honors College of

The University of Texas at Arlington in Partial Fulfillment

of the Requirements

for the Degree of

HONORS BACHELOR OF SCIENCE IN MECHANICAL ENGINEERING

THE UNIVERSITY OF TEXAS AT ARLINGTON

May 2019

ACKNOWLEDGMENTS

I would like to thank Dr. Raul Fernandez, Dr. Yawen Wang and Dr. Hullender for their support and mentorship throughout this project. This project could not have been completed without their input and hours of assistance. I would also like to thank those on my senior design team: Joseph Herring, Tim Pugliese, Jacob Lamotte-Dawaghreh, Logan Pechal, and Garrett Tolar. They have been a joy to work with this past year. Finally, I would like to thank my family and friends, including the Honors College faculty. Without their continual support, encouragement, and guidance, this project would not have been possible.

May 3, 2019

ABSTRACT

STEERING AND SUSPENSION DESIGN

FOR AN EFFICIENT ELECTRIC

DRIVE SYSTEM

Matthew Smith, ME

The University of Texas at Arlington, 2019

Faculty Mentors: Raul Fernandez and Yawen Wang

As the effects of climate change have left the horizon and become a present-day problem, the transportation industry is aggressively seeking to reduce harmful emissions. The majority of cars currently on the road are powered by a central engine connected to two or four wheels through a transmission driveshaft(s), and other mechanical linkages. Each of these components, however, introduces significant inefficiencies and can result in let power losses upwards of 15%. By replacing the central motor with four smaller motors placed inside the wheel hubs, these mechanical inefficiencies can be eliminated. This project develops a conceptual steering and suspension system to accommodate the inclusion of a drive motor inside the wheel hub. Additionally, a quarter car analysis was used to determine the necessary spring and damping rates for optimal ride comfort.

TABLE OF CONTENTS

LIST OF FIGURES

LIST OF TABLES

CHAPTER 1

INTRODUCTION

1.1 In-Wheel Drive Systems

Climate change has prompted the transportation industry to aggressively pursue reducing its carbon emissions. Engines and drivetrains are constantly refined to gain fractional increases in efficiency. Thus, every improvement to the current system is invaluable. One major source of power loss in modern systems is the drivetrain, which consists of everything between the output shaft from the engine to the u-joint of the axle that drives the wheel and includes the transmission and driveshaft(s). Each of these joints causes a slight loss in power. Additionally, each of these components adds a significant amount of rotating mass, which again siphons energy that otherwise could be used for propelling the car. In total, these losses can add up to more than 15% of the power output from the engine [1].

To address these inefficiencies, some have proposed eliminating these components altogether and placing the power source directly inside the hub of the wheel. These so-called in-wheel drive systems would not only regain the 15% power lost in traditional systems, but would also be electric, further reducing the overall carbon footprint.

Nevertheless, designing an in-wheel drive system doesn't come without its challenges. First, the motor must be placed where the suspension strut normally mounts. Thus, the steering knuckle and suspension joints must be redesigned to accommodate this change. Additionally, adding the motor to the wheel greatly increases the unsprung weight of the vehicle, or the weight of the components that are not isolated from the road via the suspension. This weight is traditionally kept as low as possible because lower weights is supposedly correlated with better handling. However, Lotus Engineering performed a study that proved this assumption to be a myth on the condition that the suspension is properly tuned to accommodate the weight redistribution [2]. This project aimed to develop solutions that addressed and mitigated these challenges.

1.2 Benefits of In-Wheel Drive

In addition to the efficiency gained, in-wheel drive systems allow for improved torque vectoring. Modern cars use mechanical systems to supply power to specific wheels for optimal traction. However, these systems are limited in the amount of power they can redirect and introduce further inefficiency to the system. Since the in-wheel drive has individual electric motors, however, software can be used to supply different amounts of current to each of the motors, and thus the torque supply can be completely controlled. This can greatly improve vehicle safety by supplying power to the wheels that have the most traction, maintaining superior control. Another benefit the in-wheel system offers is increased space. The area formerly occupied by the motor can be repurposed to accommodate more passengers, add storage space, or increase safety features of the car to improve impact absorption.

1.3 Project Scope

NextGen Drive, the senior design team working on this project, was tasked with designing a system that directly drives the wheels of a car via electric motors. This development included determining the performance requirements based on the customer's requirements, determining reasonable kinematics for the suspension and steering, performing a stress analysis on all necessary parts to ensure structural integrity, and finally providing the customer with a complete technical data package. In addition to these, the team decided to perform a quarter car analysis to optimize the spring and damping coefficients for passenger comfort, as well as developing a 3-D printed model for visual representation.

CHAPTER 2

PERFORMANCE REQUIREMENTS

2.1 House of Quality Analysis

At the beginning of the project, the team put together a house of quality to help translate the customer's requirements into specific technical requirements. This process is used to ensure that each of the customer's requirements (stated or implied), which tend to be more nebulous, is represented by at least one specific technical requirement. It also helps to eliminate perceived technical requirements that don't relate to any of the customer's desires for the product. It also clarifies the relationship between the numerous variables in a system, which can help quantify the trade-offs that must be made in a design. Based on the analysis performed in this project, the most heavily weighted variables were the gear ratio, motor torque, and motor RPM. The full house of quality is shown in Appendix A.

2.2 Vehicle Operational Requirements

Once the gear ratio, motor torque, and motor RPM had been designated as the preeminent parameters, an analysis was performed to quantify each of these. Table 2.1 lists the assumptions made for this analysis. Most of these regarded the geometry of the vehicle itself because the system was not designed with a specific vehicle in mind. As such, the frontal area, drag coefficient, weight, and driving conditions had to be assumed.

Table 2.1: Vehicle Dynamics Analysis Assumptions

Drag Coefficient (C_D)	0.3 [3]
Vehicle Weight (W)	4500 lbs (fully loaded)
Frontal Area (A_f)	24 ft^2
Tire Outer Diameter	30 in
Minimum Environmental Temperature	-30 °C
Maximum Environmental Pressure	102 kPa
Grade	0 to 33%

Based on these assumptions, the resistive forces, specifically the drag force, rolling resistance, and resistance due to the weight while driving up an incline were calculated using equations 1-3. The necessary power and torque to overcome these forces was then calculated for eight different scenarios, as described in Table 2.2. The results of this analysis are presented in Tables 2.3 and 2.4.

$$F_D = \frac{1}{2}\rho_{air}v_{air}^2 C_D A_f \quad (1)$$

$$F_{RR} = W \cdot f_R \cdot \cos(\theta) \quad (2)$$

$$F_W = m \cdot g \cdot \sin(\theta) \quad (3)$$

Table 2.2: Driving Conditions for the Vehicle Dynamics Analysis

Constant Velocity	Accelerating
100 mph, 0° grade	8.9 mph/s at 5 mph
85 mph, 5° grade	6.7 mph/s at 30 mph
60 mph, 8° grade	3.9 mph/s at 50 mph
30 mph, 18.4° grade	2.2 mph/s at 60 mph

Table 2.3: Motor Power Requirements

Constant Velocity	Accelerating
81.1 hp	25.4 hp
118.5 hp	132.5 hp
124.5 hp	194.8 hp
120.6 hp	220.2 hp

Table 2.4: Motor Torque Requirements

Constant Velocity	Accelerating
380 ft-lb	3234 ft-lb
741 ft-lb	2807 ft-lb
973 ft-lb	2476 ft-lb
1884 ft-lb	2333 ft-lb

2.3 Motor and Gearing Selection

Based on the performance requirements, the team set out to choose a commercially available motor and gearbox. Initially, the EMRAX 228, a brushless DC (BLDC) motor developed by the Slovenian company EMRAX, was chosen for its compact size and ability to meet the power requirements when paired with a gearbox that had a gear reduction of four. However, when the gearbox and the motor were placed inside the wheel, the system protruded a significant distance from the wheel, as can be seen in Figure 2.1(a). This was determined to no longer meet the “in-wheel” designation. Since designing a custom gear-box that would fit the geometry constraints of the application was beyond the scope of this project, a larger motor that met the performance requirements without a gearbox, the EMRAX 348, was chosen instead. This condensed the overall envelope significantly, as can be seen in Figure 2.1(b).

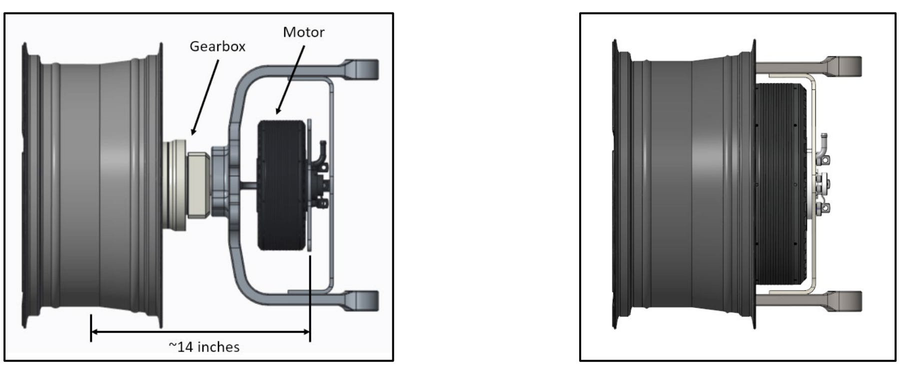

(a) (b)

Figure 2.1: (a) Initial Design with Motor and Gearbox; (b) Second Design Iteration without Gearbox

CHAPTER 3

STRUCTURAL DESIGN DEVELOPMENT

3.1 Steering Knuckle Development Process

Once the motor had been chosen, the surrounding structural components were designed. The first iteration of this design can be seen in Figure 3.1. In this design, the hub bearing was press fit onto the wheel hub, which served as the central piece for the entire system. The brake rotor, caliper, and wheel rim would bolt onto the lug nuts that protruded from the wheel hub. On the other side, the hub bearing was connected to the steering knuckle, which held the motor mount. Finally, the axle from the motor would mate with the wheel hub via a machined multi-point star pattern. Of the parts in this iteration, only the steering knuckle and motor mount were custom designed. Each of the other parts were commercially available.

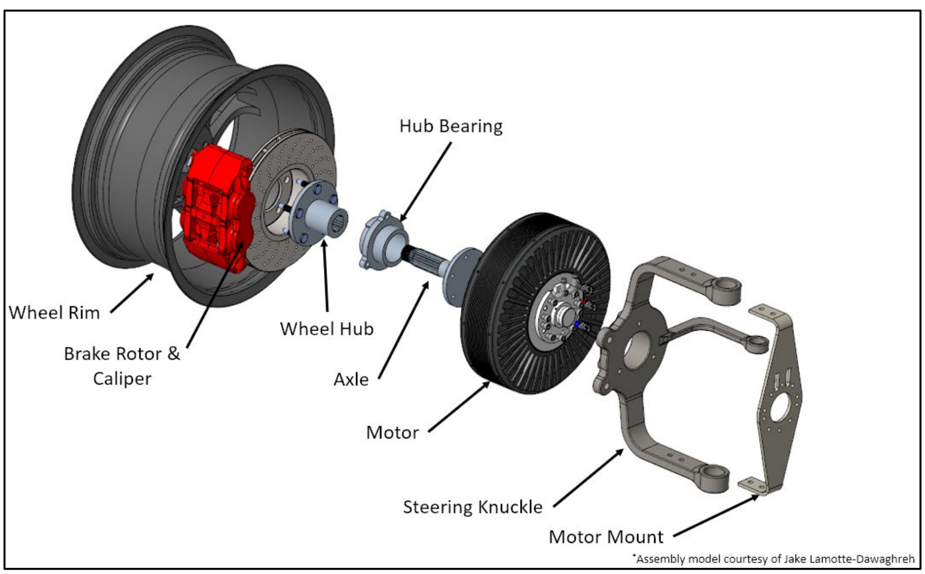

Figure 3.1: First Iteration of the In-Wheel System Design

Upon submitting this design for review, however, an issue with the steering axis was raised. For optimal handling, the steering axis should be as close to the center of the wheel as possible. This minimizes the amount of slipping between the tire and the road when the driver turns the steering wheel. The steering axis in the first iteration, however, was several inches outside of the wheel, as can be seen in Figure 3.2. Thus, the steering knuckle had to be redesigned.

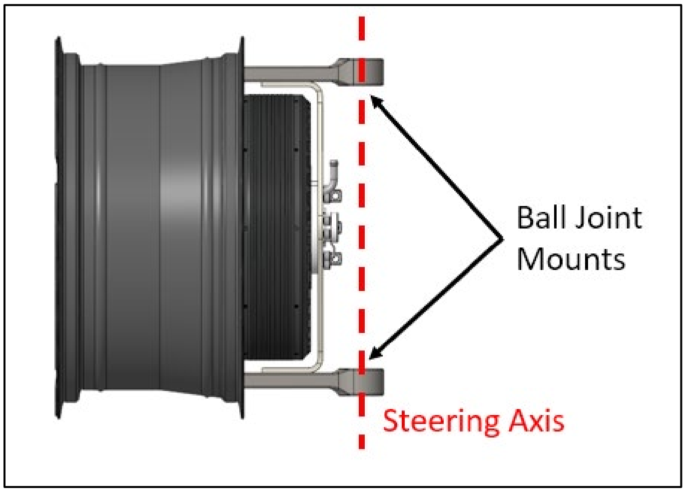

Figure 3.2: Steering Axis in the First Iteration Design

In the first iteration, two ball joints were used to combine the pivot points for the steering with the pivot points for the suspension. To prevent the suspension control arms from interfering with the motor, however, these joints had to be split into two pin joints each. This divided the knuckle into three separate pieces: two elbows and a new, smaller knuckle (see Figure 3.3). This allowed the steering axis to move toward the center of the wheel while avoiding interference between the suspension control arms and the motor.

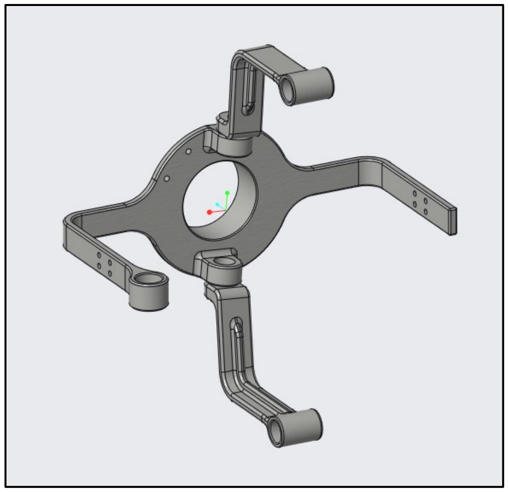

Figure 3.3: Second Iteration Steering Knuckle and Elbows

A section view of this second iteration shows the new steering axis achieved.

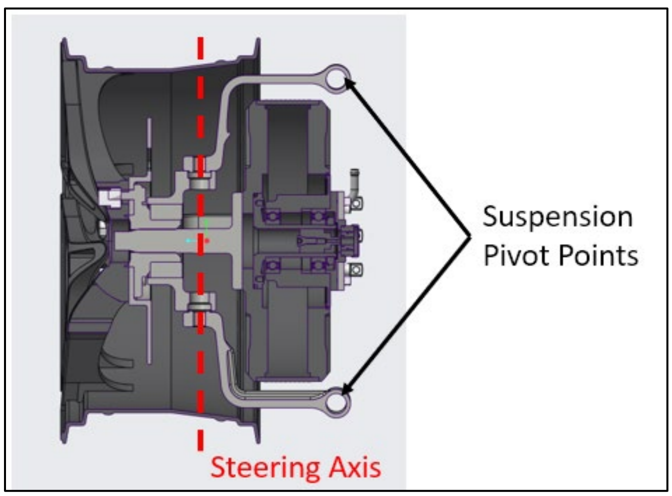

Figure 3.4: Steering Axis and Suspension Pivots in the Second Iteration Design

Figure 3.3 also shows that an extra horizontal arm was added to the new steering knuckle. This arm connected to the new motor mount that was now also oriented horizontally to allow the motor to rotate with the wheel during steering. Figure 3.5 shows an exploded view of the complete second iteration design.

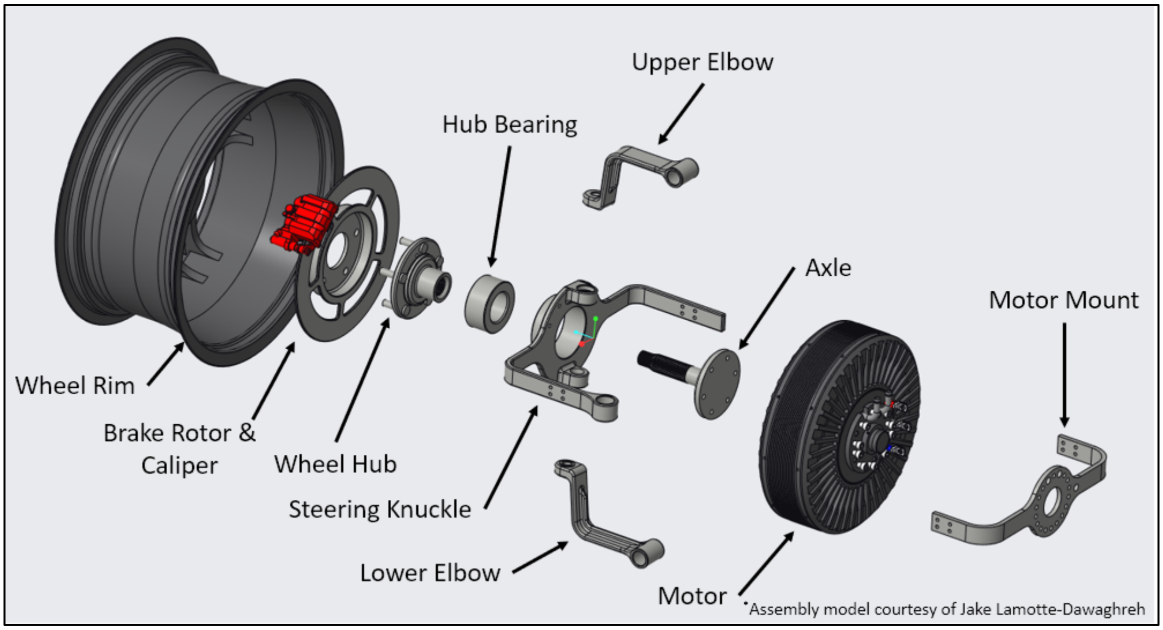

Figure 3.5: Exploded View of the Complete Second Iteration Design

Another design characteristic that a reviewer addressed was the size of the brake rotor and caliper in the first iteration. As mentioned before, these parts were commercially available for use on cars with conventional drive systems. The reviewer pointed out that the use of a BLDC motor, such as the EMRAX 348, allowed for the implementation of regenerative braking, where some of the car's kinetic energy can be used to drive the motor in reverse and recharge the car's battery. Thus, through some simple software in the motor controller, 70% to 80% of the cars kinetic energy can be removed without a friction brake. This meant that the brake rotor and caliper could be resized to have 30% of the original frictional contact area, making the components much smaller.

The final adjustment made between the first and second iterations was to include a caster angle. Caster is one of three alignment specifications in cars. It functions on the same principle as the front wheels of a shopping cart. Since the contact point between the wheel and the ground is behind the intersection of the steering axis and the ground, a moment is generated around the steering axis that forces the wheel back in line with the direction of travel. In a car, this angle determines how hard it is to turn the steering wheel into a turn and how quickly the steering wheel returns to straight if allowed to freely rotate out of a turn. In the second iteration of the design, a standard caster angle of five degrees was added to the surfaces between the steering knuckle and the elbows. This angle is described graphically in Figure 3.6 below. Once the caste angle had been added, the design concept was finalized, and the parts were passed on to the rest of the senior design team for stress analysis.

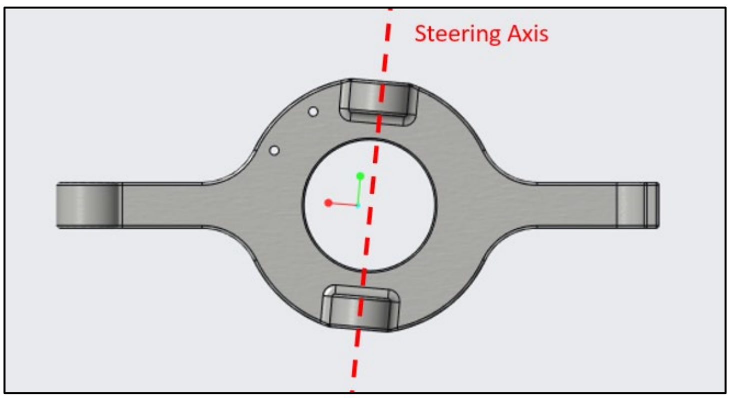

Figure 3.6: Caster Angle in the Steering Axis

CHAPTER 4

QUARTER CAR SUSPENSION ANALYSIS

4.1 Analysis Process

While the rest of the team was performing the stress analysis, this project began focusing on developing a quarter car suspension analysis to determine the optimal spring and damping coefficients for a theoretical shock that would minimize the vibration of the car for maximum passenger comfort. Since the motor now occupied the space where the suspension strut would have normally mounted in a traditional MacPherson strut or double a-arm suspension system, it was decided that a rocker arm suspension would be used (see Figure 4.1).

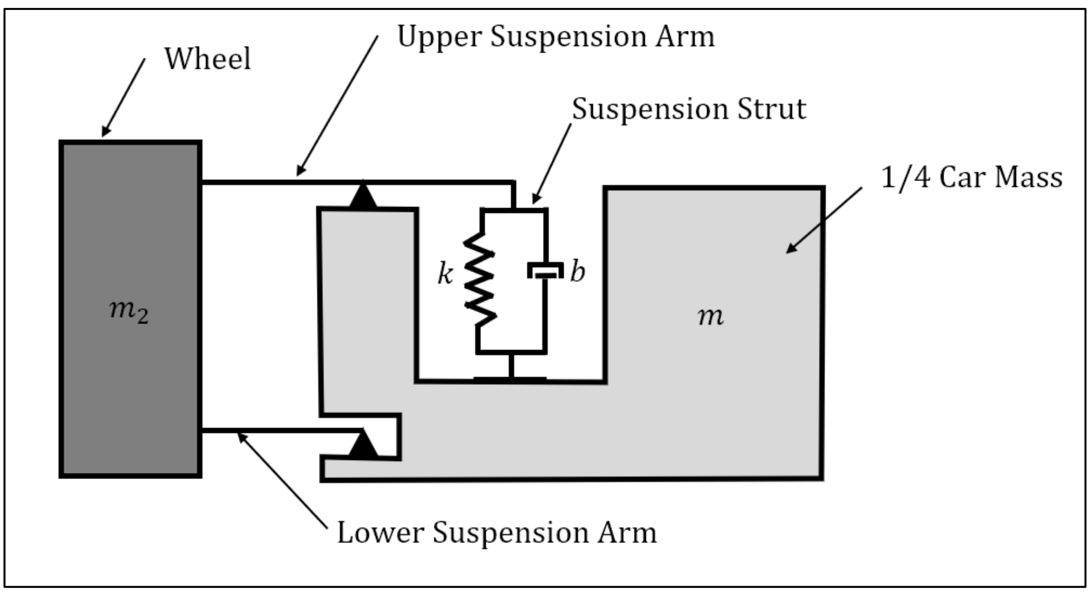

Figure 4.1: Rocker Arm Suspension Diagram

For the purposes of this analysis, it was assumed that the tire maintained perfect contact with the road, that the body of the car didn't rotate, and that the input was stochastic and continuous. The assumption that the tire maintained perfect contact with the road meant that the mass of the tire became irrelevant since it would be displaced the same amount regardless of the mass. This resulted in the following free body diagram (FBD):

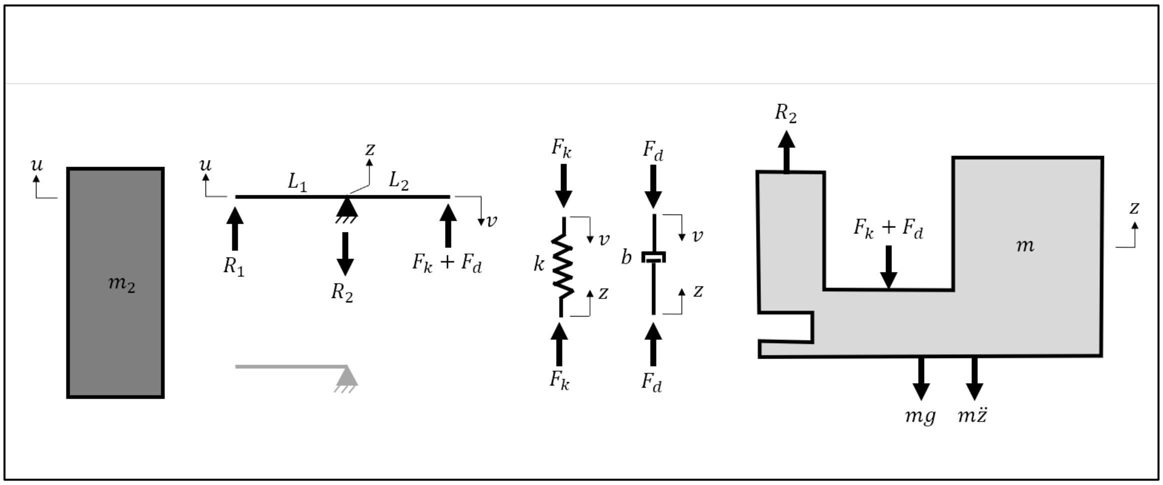

Figure 4.2: Suspension Free Body Diagram (FBD)

The FBD was then used to develop the system model equations as follows:

$$v = \frac{L_1}{L_2}u - \left(\frac{L_1 - L_2}{L_1}\right)z \tag{4}$$

$$r = \left(\frac{L_2}{L_1}\right)^2 \tag{5}$$

$$F_k + F_d + R_1 - R_3 = 0 \tag{6}$$

$$F_k = k(v + z) + \left(\frac{mg}{2}\right)r \tag{7}$$

$$F_d = b(\dot{v} + \dot{z}) \tag{8}$$

$$m\ddot{z} + mg + 2(F_k + F_d - R_3) = 0 \tag{9}$$

Finally, the transfer function for the displacement of the car was obtained in terms of the displacement input. That transfer function is presented here:

$$F(s) = \frac{bs + k}{\frac{m}{2}\left(\frac{L_1}{L_2}\right)^2 + bs + k} \tag{10}$$

Combining this transfer function with the input PSD transfer function and adding a filter to attenuate the response above the maximum relevant frequency gives:

$$F_{\ddot{z}}(s) = \frac{2\pi\sqrt{Av}(bs^2 + ks)}{\frac{m}{2C}\left(\frac{L_1}{L_2}\right)^2 + \left[\frac{m}{2}\left(\frac{L_1}{L_2}\right)^2 + \frac{b}{C}\right]s^2 + \left(\frac{k}{C} + b\right)s + k} \tag{11}$$

where C is the filter frequency in radians per second. The mean square value of the PSD was then calculated using the tables in Dr. David Hullender's [4] book using symbolic math in MATLAB. Finally, a series of spring and damping coefficients were passed through the symbolic function and the minimum root mean square value of the car vibration ($\ddot{z}$) was used to choose the optimum coefficients. This approach, however, failed to consider alternative optimization goals or system constraints, such as keeping the suspension from bottoming out, achieving an acceptable settling time, or maintaining contact with the road. Thus, the "optimization" process simply selected the minimum spring and damping coefficients used in the simulation since those would result in the smallest mean acceleration.

4.2 Analysis Results

The minimum values passed into the simulation were a spring constant of 10,000 N/m and damping coefficient of 500 Ns/m. These values resulted in the following time response given an impulse input of 5 cm (see Figure 4.3). The full optimization code is presented in Appendix B.

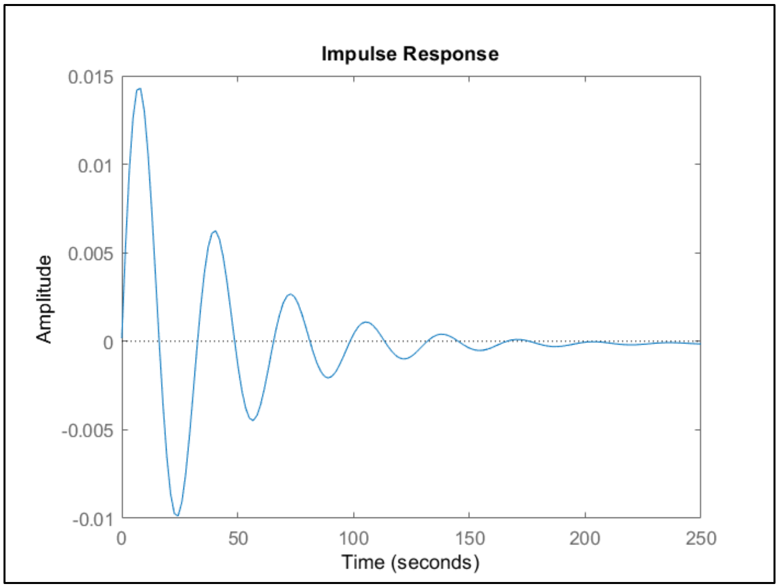

Figure 4.3: Time Response of the System Given k = 10,000 N/m and b = 500 Ns/m

As can be seen, the system takes almost four minutes to reach steady state, but the amplitude of the acceleration is only 0.015 m/s, or 0.0015 g's, which is well below the comfort threshold of 0.08 g's.

CHAPTER 5

CONCLUSIONS

5.1 Results from Current Project

This project showed that an in-wheel drive system is an attractive alternative to conventional drive systems due to its increase in overall efficiency, improved safety through torque vectoring, and increased cabin space. Not only does it eliminate numerous mechanical inefficiencies present in standard drivetrains, it also utilizes electric motors rather than an internal combustion engine, greatly reducing the carbon footprint. Additionally, the potential safety of the vehicle is significantly greater than conventional vehicles due to the improved torque vectoring capabilities and the opportunity to utilize the regained space for additional safety features. Nevertheless, the specific concept developed in this project would greatly benefit from some additional work to become an optimal design.

5.2 Recommendations for Further Work

The first and possibly most important change would be to use a custom designed motor that is tuned to meet the power and torque requirements and has an integrated hub bearing. This would significantly reduce the size of the motor and increase the design envelope for the remaining components. Not only does this have positive implications for the overall weight of the system, but it would also allow for structural component shapes that would better meet the loading conditions of the vehicle.

The second recommended improvement would be to design a custom gearbox to pair with the new custom designed motor. Most BLDC motors are more efficient at higher RPMs and lower torques. Thus, designing a custom gearbox that would meet the geometric constraints of this system would allow the motor to operate at ideal efficiencies while meeting and exceeding performance requirements.

The third component that could be further developed would be the suspension analysis. The analysis performed only considered the vibration experienced by the car passengers in its optimization. This, however, reduced the problem from an optimization problem to a pure minimization. As such, to obtain truly optimized spring and damping coefficients, other optimization parameters such as the stroke of the suspension, the desired time response of the system, and the tire contact with the road based on a spring-damper-modelled tire should also be considered.

Finally, many of the structural components could be improved for stress through what is known as topology analysis. This analysis would identify the loading path of the system and determine the shape of the structural components that resulted in the lightest part while maintaining all necessary safety factors and remaining within the geometric design envelope.

Should these changes be incorporated, the resulting system would provide stiff competition against current conventional drive systems.

APPENDIX A

HOUSE OF QUALITY

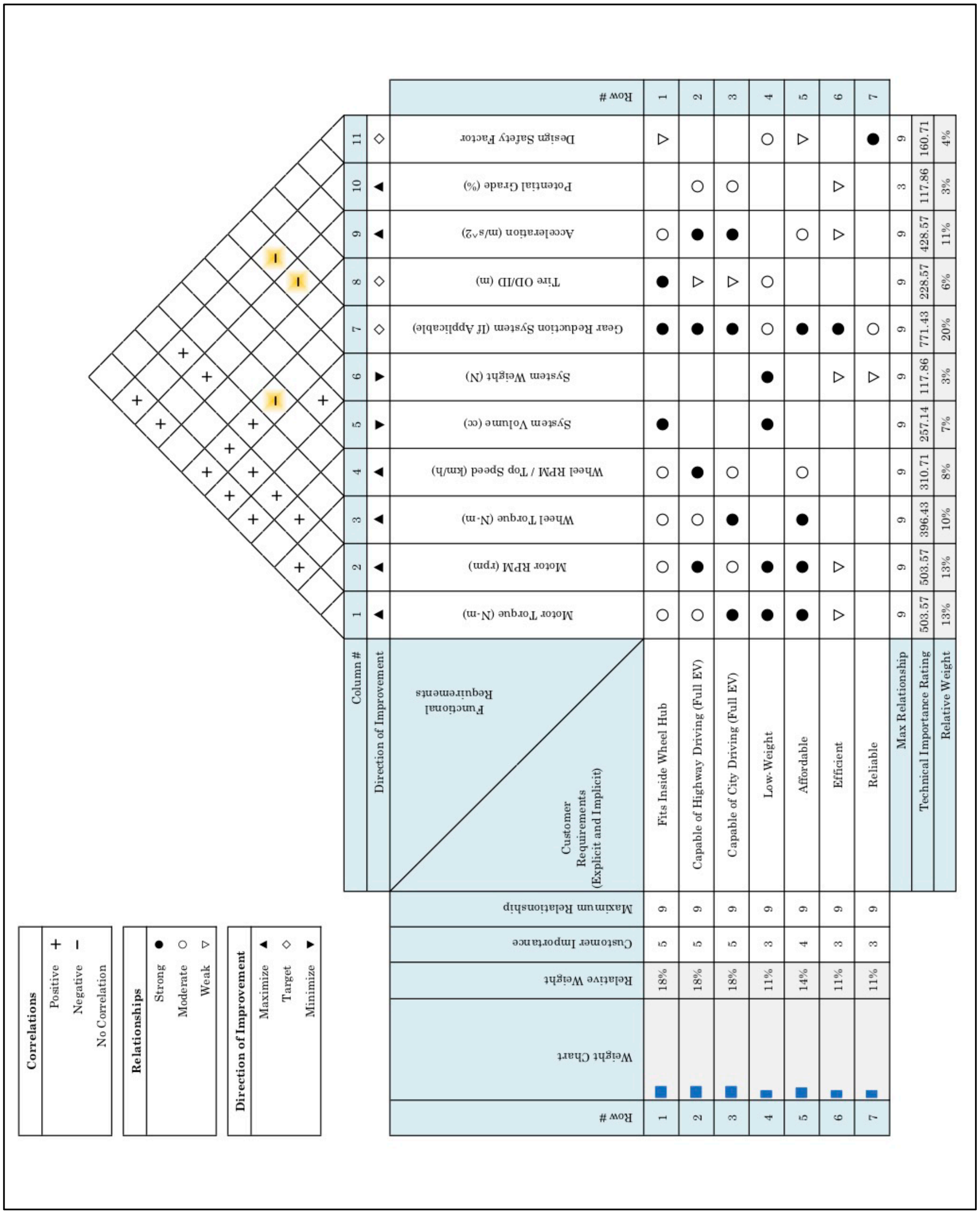

Figure A.1 House of Quality Analysis

APPENDIX B

QUARTER CAR ANALYSIS MATLAB CODE

```
g = 9.81; %ft/s^2
L1 = 10; %in
L1 = L1 * .0254; %converts to meters
L2 = 11; %in
L2 = L2 * .0254; %converts to meters
v = 1056; %in/s
v = v * 0.0254; %m/s
m1 = 55; %kg
m = 455*2; %kg

lmin = 2.5; %minimum feature size (in); based on contact patch of
tire
lmin = lmin * 0.0254; %converts to m
fmax = v/lmin %maximum input frequency
H = 1/(2*fmax); %time interval; input for PSD function
r = (L1/L2)^2;

% a = 4.8 * 10^-7; %smooth highway
a = 4.4 * 10^-6; %highway with gravel


C = fmax; %upper limit of filter

kinit = 10000;
kfin = 100000;
binit = 500;
bfin = 5000;
kmat = kinit : kinit : kfin; %spring constants (N/m)
%https://www.engineeringtoolbox.com/hookes-law-force-spring-con-
stant-d_1853.html
bmat = binit : binit : bfin; %damping coefficients (Ns/m)
%see pg. 6 (labeled pg. 40) http://transportprob-
lems.polsl.pl/pl/Archiwum/2011/zeszyt2/2011t6z2_05.pdf
[~,P] = size(kmat);
[~,Q] = size(bmat);

syms b k c0 c1 c2 d0 d1 d2 d3 Zddms

c0 = 0;
c1 = 2*pi*sqrt(a*v)*k;
c2 = 2*pi*sqrt(a*v)*b;

d0 = k;
d1 = (k/C + b);
d2 = (m*r/2 + b/C);
d3 = m*r/(2*C);

Zddms = (0.5)*(c2^2*d0*d1 + (c1^2 - 2*c0*c2)*d0*d3 +
c0^2*d2*d3)/(2*d0*d3*(-d0*d3 + d1*d2));
%from Dr. Hullender's Notebook, p. 141

t = 0;
```

```
for p = 1:P
    k = kmat(p);
    for q = 1:Q
        t = t+1;
        b = bmat(q);
        c0hold = double(subs(c0));
        c1hold = double(subs(c1));
        c2hold = double(subs(c2));

        d0hold = double(subs(d0));
        d1hold = double(subs(d1));
        d2hold = double(subs(d2));
        d3hold = double(subs(d3));

        ZTF = tf([c2hold c1hold c0hold],[d0hold d1hold d2hold
d3hold]);
        evals(t,:) = eig(ZTF)';
        Zddms_hold = subs(Zddms);
        ZDDMS(p,q) = double(Zddms_hold);

        if ZDDMS(p,q) < 0
            ZDDMS(p,q) = 10e9; %negative mean square values are
meaningless
        end
    end
end

ZDDRMS = sqrt(ZDDMS);
[minaccelvec, I1] = min(ZDDRMS);
[minaccel, I2] = min(minaccelvec);

optB = bmat(I2);
optK = kmat(I1(I2));

b = optB
k = optK

c0hold = double(subs(c0));
c1hold = double(subs(c1));
c2hold = double(subs(c2));

d0hold = double(subs(d0));
d1hold = double(subs(d1));
d2hold = double(subs(d2));
d3hold = double(subs(d3));

ZTF = tf([c2hold c1hold c0hold],[d0hold d1hold d2hold d3hold]);

figure
impulse(.05*ZTF)
figure
nyquist(ZTF)
```

```
figure
rlocus(ZTF)

sag = 4; %allowable spring sag under weight of car (in)
sag = sag*0.0254;
kreal = (m/2)*g/sag; %more realistic k value
```

REFERENCES

[1] “Drivetrain losses (efficiency),” X-engineer.org, URL: https://x-engineer.org/automotive-engineering/drivetrain/transmissions/drivetrain-losses-efficiency/, retrieved 29 January 2019.

[2] R. Schreiber, “Heresy Unspring, Lotus Engineering: Unsprung Weight Doesn’t Really Matter Much,” 19 April 2013, The Truth About Cars, URL: https://www.thetruthaboutcars.com/2013/04/heresy-unsprung-lotus-engineering-unsprung-weight-doesnt-really-matter-much/, retrieved 29 January 2019.

[3] Yawen Wang, Powertrain Design and Analysis, Lecture 3 Vehicle Longitudinal Dynamics

[4] Hullender, D. (2017). Dynamic Systems Modeling and Simulation Theory and Examples.

BIOGRAPHICAL INFORMATION

Matthew Smith is an undergraduate student at the University of Texas at Arlington planning to graduate with an Honors Bachelor of Science in Mechanical Engineering in May of 2019.

He entered UTA as an Honors Distinction Scholar in the Honors College and has been involved as an Honors College Advocate and an Honors College Office Assistant. In addition to completing his Senior Project, he had the opportunity to participate in research under Dr. Frank Lu at the Aerospace Research Center and under Dr. Sunand Santhanagopalan in the Multi-Scale Energy Systems Laboratory. He also spent the summers after his sophomore and junior years interning at Lockheed Martin Missiles and Fire Control in Grand Prairie, Texas.

Upon matriculation, Matthew plans to begin working in the aerospace and defense industry while pursuing his M.S. in Mechanical Engineering at UTA. He also plans to pursue an MBA in the future.